Neurosci Bull February 1, 2014, 30(1): 43–52. http://www.neurosci.cn
DOI: 10.1007/s12264-013-1373-4

·Original Article·

Blockade of Na^+/H^+ exchanger type 3 causes intracellular acidification and hyperexcitability *via* inhibition of pH-sensitive K^+ channels in chemosensitive respiratory neurons of the dorsal vagal nucleus in rats

Jing Zhang[1], Hui Peng[2], Sigrid C. Veasey[3,4], Jing Ma[1], Guang-Fa Wang[1], Ke-Wei Wang[2]

[1]*Department of Respiratory and Critical Care Medicine, Peking University First Hospital, Beijing 100034, China*

[2]*Departments of Neurobiology and Molecular and Cellular Pharmacology, Peking University Health Science Center, Beijing 100034, China*

[3]*Center for Sleep and Circadian Neurobiology,* [4]*Department of Medicine, University of Pennsylvania School of Medicine, Philadelphia, Pennsylvania, USA*

Corresponding authors: Jing Ma and Guang-Fa Wang. E-mail: majjmail@163.com; wangguangfa@hotmail.com

ABSTRACT

Extracellular pH (pH_e) and intracellular pH (pH_i) are important factors for the excitability of chemosensitive central respiratory neurons that play an important role in respiration and obstructive sleep apnea. It has been proposed that inhibition of central Na^+/H^+ exchanger 3 (NHE-3), a key pH_i regulator in the brainstem, decreases the pH_i, leading to membrane depolarization for the maintenance of respiration. However, how intracellular pH affects the neuronal excitability of respiratory neurons remains largely unknown. In this study, we showed that NHE-3 mRNA is widely distributed in respiration-related neurons of the rat brainstem, including the dorsal vagal nucleus (DVN). Whole-cell patch clamp recordings from DVN neurons in brain slices revealed that the standing outward current (I_{so}) through pH-sensitive K^+ channels was inhibited in the presence of the specific NHE-3 inhibitor AVE0657 that decreased the pH_i. Exposure of DVN neurons to an acidified pH_e and AVE0657 (5 μmol/L) resulted in a stronger effect on firing rate and I_{so} than acidified pH_e alone. Taken together, our results showed that intracellular acidification by blocking NHE-3 results in inhibition of a pH-sensitive K^+ current, leading to synergistic excitation of chemosensitive DVN neurons for the regulation of respiration.

Keywords: Na^+/H^+ exchange; potassium channel; dorsal vagal nucleus; *in situ* hybridization; respiration

INTRODUCTION

Obstructive sleep apnea affects >2% of the general population, and is an independent risk factor for cardiovascular morbidity and mortality[1]. Recent studies support the concept that impaired central chemosensitivity not only occurs in patients with central sleep apnea and multiple system atrophy, but also contributes to a worsened oxygen desaturation index in patients with obstructive sleep apnea[2, 3].

Many brainstem regions contribute to central chemoreception, including the dorsal vagal nucleus (DVN), nucleus tractus solitarius (NTS)[4-7], ventrolateral medulla[8], medullary raphe[9], pre-Bötzinger region[10], retrotrapezoid nucleus (RTN)[11], and locus coeruleus[12]. In these regions, subsets of neurons are depolarized in response to increased levels of CO_2, as well as decreased intracellular pH (pH_i) or extracellular pH (pH_e). The depolarization response is maintained in the absence of chemical synaptic transmission, suggesting that direct chemosensitivity

is involved in the response[5]. Previous studies have indicated that the excitability of chemosensitive neurons is closely related to pH_i[13, 14]. However, how pH_i participates in respiratory chemical control and whether there is any relationship (additive, synergistic, or even subtractive) between pH_i and pH_e remain unclear.

Sodium proton exchanger 3 (NHE-3) mediates pH_i recovery from acidification in most chemosensitive neurons and may determine their excitability by adjusting pH_i[15, 16]. Selective inhibition of NHE-3 *in vivo* stimulates the central respiratory system[17], increases minute ventilation[18], and facilitates a low system loop gain[19], indicating a potential for specific NHE-3 inhibitors in the treatment of obstructive sleep apnea.

In the present study, we investigated the central distribution of NHE-3 mRNA in respiratory neurons, and the mechanism underlying the enhanced hyperexcitability of DVN neurons induced by extracellular acidification plus the specific NHE-3 blocker AVE0657.

MATERIALS AND METHODS

Pharmacological Agents

AVE0657 was a generous gift from Sanofi-Aventis Pharmaceuticals (Frankfurt am Main, Germany). This is a novel inhibitor of Na^+/H^+ exchangers, with greater selectivity for type 3 than type 1. Consistent with other specific inhibitors of NHE-3[15, 16], our preliminary studies showed that AVE0657 affects pH_i without affecting pH_e. The stock solution of AVE0657 (10 mmol/L) was prepared in DMSO, which was added to ACSF directly (the highest final concentration of DMSO used was 0.05%).

Animals

Sprague-Dawley rats were housed under a 12:12 h light/dark cycle with free access to food and water. Brain sections and slices were obtained from 250–350 g adult and neonatal rats (7–12 days postnatal), respectively. All the procedures were in accordance with Peking University First Hospital Institutional Animal Care and Use Committee guidelines and were approved by the Committee (J201113).

In situ Hybridization

Rats were anesthetized with sodium pentobarbital followed by transcardial perfusion with 4% paraformaldehyde. Brains were harvested, cryoprotected, sectioned and processed as previously described[20].

A commercial *in situ* hybridization kit was used (Tianjin Haoyang Biological Manufacture Co., Ltd., Tianjin, China). The sequence of the oligonucleotide anti-sense probe of NHE-3 was: 5'-ACTGAGG-AAGACACCATAGAGGGACAATC-3'. This probe was analyzed and 3'-end labeled with digoxigenin by nick translation. The sense probe was used as a control. *In situ* hybridization was performed according to the manufacturer's protocol. Sections were stained with DAB-nickel, counterstained with Harris hematoxylin, dehydrated and mounted. All slides were viewed under an Olympus AX70 photomicroscope and images captured by a digital camera.

Dorsal Vagal Nucleus (DVN) Slice Preparation

For dye-loading and electrical recordings from DVN neurons, brainstem slices were prepared from neonatal rats. The animals were rapidly decapitated and the brainstem removed. Slices (300 μm) were cut on a vibratome (Leica 1000) in an ice-cold, oxygenated (95% O_2 and 5% CO_2) artificial cerebrospinal fluid (ACSF) with sucrose (in mmol/L: 260 sucrose, 3 KCl, 5 $MgCl_2$, 1 $CaCl_2$, 1.25 NaH_2PO_4, 26 $NaHCO_3$, 10 glucose, 1 kynurenic acid)[21], incubated for 1 h at 34°C, and then at room temperature in standard ACSF (in mmol/L: 3 KCl, 1 $MgCl_2$, 2 $CaCl_2$, 1.25 NaH_2PO_4, 26 $NaHCO_3$, 124 NaCl, 10 glucose equilibrated with 95% O_2 and 5% CO_2, pH 7.4).

Measurement of pH_i in Slices

The measurement of pH_i was modified from the method established by Ritucci *et al.*[22], using a confocal microscope (TCS SP5, Leica). Slices were incubated in standard ACSF equilibrated with 95% O_2 and 5% CO_2 containing 25 μmol/L 2',7'-biscarboxyethyl-6-carboxyfluoresce in acetoxymethyl ester (BCECF-AM, Molecular Probes/Invitrogen, Eugene, OR) at room temperature for 20 min in the dark. Individual slices were placed in a dish and immobilized with a grid made of nylon fibers held on a U-shaped platinum frame. The dish was placed on the stage of an upright Leica microscope.

BCECF-loaded DVN neurons were alternately excited with laser lines at 458 nm and 496 nm. Emitted fluorescence ranging from 520 nm to 580 nm was imaged

by the confocal microscope. Image acquisition was repeated at 40–60 s intervals to reduce photo-bleaching. Calibration curves for BCECF in individual neurons were made with high-K^+ nigericin solution (in mmol/L: 104 KCl, 1.3 $MgSO_4$, 1.25 KH_2PO_4, 25 NMDG-HEPES, 25 K-HEPES, 10 glucose, 2 $CaCl_2$, and 0.004 nigericin; titrated with either KOH or HCl to pH values ranging from 6.6 to 7.8). All pH_i measurements were made from the neuron soma. The fluorescence images at 458 nm and 496 nm excitation and the 496:458 ratio (R_{fl}) were analyzed by LAS AF (TCS SP5, Leica).

Electrophysiological Recordings

Brain slice recordings were made at room temperature in HEPES-buffered ACSF (H-ACSF) (in mmol/L: 3 KCl, 1 $MgCl_2$, 2 $CaCl_2$, 1.25 NaH_2PO_4, 15 HEPES, 124 NaCl, and 10 glucose, pH adjusted to desired levels using NaOH) perfused at 4–5 mL/min, and gassed continuously with 100% O_2. Patch electrodes were pulled from borosilicate capillaries and fire-polished to a resistance of 3–6 MΩ. Electrodes were filled with buffered pipette solution (in mmol/L: 120 KCH_3SO_3, 1 $MgCl_2$, 0.5 $CaCl_2$, 4 NaCl, 10 HEPES, 10 EGTA, 3 MgATP, 0.3 GTP-Tris, pH 7.3) or unbuffered pipette solution (in mmol/L: 120 KCH_3SO_3, 1 $MgCl_2$, 0.5 $CaCl_2$, 4 NaCl, 10 EGTA, 3 MgATP, 0.3 GTP-Tris, at 310 mOsmol/L and pH 7.3, adjusted with mannitol and KOH)[23].

DVN neurons were identified by their large fusiform shape and anatomical location dorsal to the central canal with infrared differential interference optics (Olympus, Japan). Whole-cell recordings were obtained using an Axopatch 700B amplifier and patch-clamp software (Axon Instruments). In voltage-clamp recordings, the membrane properties were monitored with a 750-ms hyperpolarizing voltage ramp from a holding potential of −20 to −120 mV or recorded continuously in gap free mode. Current-clamp recordings were made in the absence of any holding currents. The liquid junction potential (~10 mV) was corrected off-line. Analysis was performed with Clampfit 10.0. Statistical comparisons were carried out using the paired *t*-test, and $P < 0.05$ was regarded as statistically significant. Results are presented as mean ± SEM, with "*n*" indicating the number of cells. Fitting with the Goldman-Hodgkin-Katz equation was performed using Clampfit 10.0 with the Levenberg-Marquardt method. Full data sets were obtained from 40 brain slices. For pH_e and drug experiments, each slice was exposed only once to acidified/alkalized H-ACSF or the drug.

RESULTS

Expression of NHE-3 in Rat Brainstem

The expression of NHE-3 mRNA in adult rat brainstem was examined using *in situ* hybridization. Three coronal levels of the brainstem that are rich in neurons with chemosensitive receptors were examined: caudal medulla, rostral medulla and caudal pons[24]. At the level of the caudal medulla, the DVN and NTS were labeled with antisense probe (Fig. 1A). Neurons within the pre-Bötzinger region were also labeled with NHE-3 antisense RNA. At the level of the rostral medulla, NHE-3 mRNA was detected in the medullary raphe (Fig. 1B). Also at this level, RTN neurons showed positive labeling. The mesencephalic trigeminal nucleus, labeled as triangular in shape, showed high NHE-3 mRNA levels, as did the motor trigeminal nucleus (Fig. 1C).

We also checked other chemosensitive brainstem regions and respiration-related motor nuclei. Very weak staining was detected in the locus coereleus, while no signal was found in the hypoglossal nucleus (XII) (Fig. 1A), Kolliker-Fuse nucleus, and parabrachial nucleus.

In light of the NHE-3 localization, we chose DVN, a key nucleus with chemosensitive receptors and expressing both NHE-3 and TASK channels[25], for the following studies.

Effects of AVE0657 on pH_i in DVN Neurons

In 300-μm thick slices, we were able to visualize cells within 30 μm of the slice surface, and many large cell bodies were successfully loaded with dye (Fig. 2A–C). First, we made a calibration curve for BCECF fluorescence using the high-K^+/nigericin technique in the DVN. This was done by manual control of R_{fl} values close to 1 at pH 7.2, and then we calculated other R_{fl} values at different pH values (ranging from 6.6 to 7.8) under the same experimental conditions. A calibration equation of R_{fl} *versus* pH_i was then constructed[26]: $R_{fl} = 0.6377\ pH_i - 3.55$ ($R^2 = 0.98$, $n = 105$) (Fig. 2D).

We found that the initial pH_i value for the DVN neurons in H-ACSF (pH_e 7.4 at 28°C) was 7.46 ± 0.005 ($n = 52$). Once exposed to 5 μmol/L AVE0657, the pH_i values fell rapidly. After 1–2 min, the pH_i value was stable at 7.3 ± 0.008

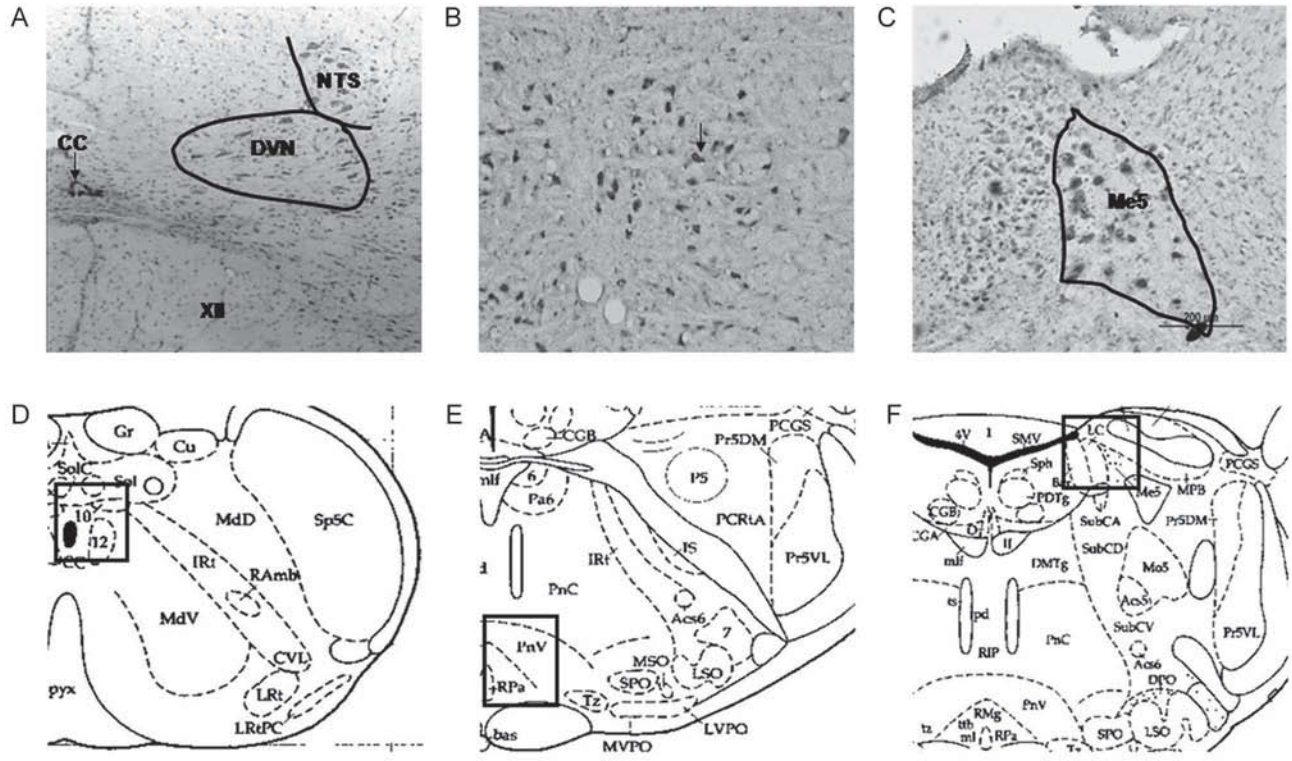

Fig. 1. NHE-3 mRNA expression in main chemosensitive neurons. A–C: NHE-3 mRNA was expressed in the NTS and DVN (A, bregma 14.6 mm), medullary raphe (B, bregma 10.04 mm), and Me5 (C, bregma 9.8 mm), while no NHE-3 signal was found in XII (A). D–F: Schematic drawings adapted from The Rat Brain in Stereotaxic Coordinates (Paxinos and Watson). The brain regions of panels A–C are indicated by the square boxes in panels D–F, respectively. CC, corpus callosum; DVN, dorsal vagal nucleus; NTS, nucleus tractus solitarius; Me5, mesencephalic trigeminal nucleus; XII, hypoglossal motor nucleus. Scale bar, 200 μm.

(n = 32), and no recovery occurred (Fig. 2E). But AVE0657 at 2 μmol/L (n = 11) had no effect on pH_i (data not shown), as compared with vehicle alone (0.05% DMSO, n = 9) (Fig. 2F).

Modulation of I_{so} by pH_e

As in previous studies[27, 28], we used buffered pipette solution referred to gap free current when the cell membrane potential was held at −20 mV as the standing outward current (I_{so}). Without exception, acidification of pH_e from 7.4 to 6.5 resulted in a reduction of I_{so} from 177 ± 40 pA to 101 ± 44 pA in 6 min (P <0.01, paired t-test; n = 6; Fig. 3A, B, D and F), whereas alkalization of pH_e from 7.4 to 8.2 induced a corresponding increase of I_{so} from 177 ± 40 pA to 306 ± 80 pA (P <0.01, paired t-test; n = 6; Fig. 3A, C, D and F). Analysis of the current-voltage (I-V) relations, obtained by applying hyperpolarizing voltage ramps from −20 to −120 mV, revealed an increase in conductance at pH_e 8.2 and a decrease at pH_e 6.5 (Fig. 3D). Subtraction of the I-V relationships at pH_e 8.2 and 6.5 showed that the pH_e-sensitive current reversed at −88 ± 4 mV (n = 6), close to the predicted K^+ equilibrium potential (E_k) of −90 mV. Furthermore, the subtracted I-V relationships were well-fitted by the Goldman-Hodgkin-Katz equation[29].

Effects of AVE0657 on I_{so} and Firing Rate

In this part, all the recordings were carried out in spontaneously-active DVN neurons. Before application of AVE0657, the average control values under normal conditions (pH_e 7.4) were −53.4 ± 2.8 mV for membrane potential and 1.9 ± 0.3 Hz (n = 21) for firing rate. A representative recording of the electrophysiological response to AVE0657 is shown in Fig. 4A. Application

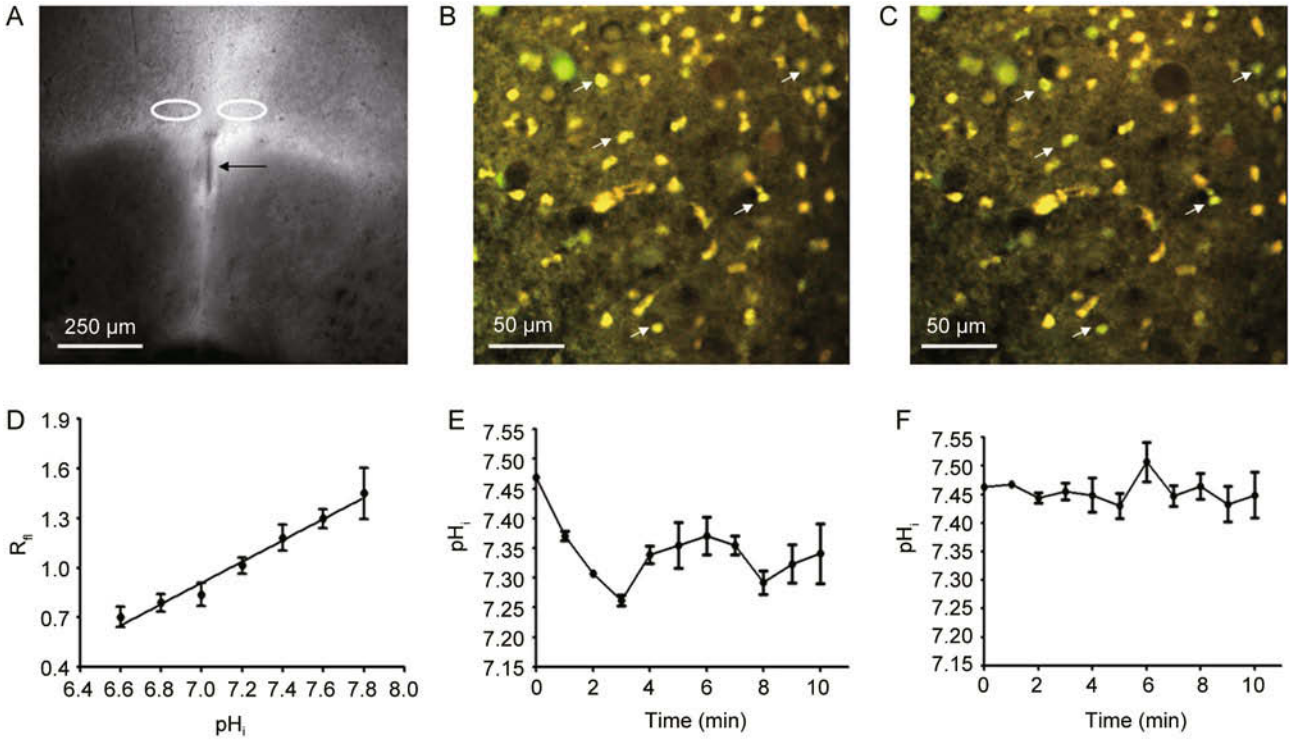

Fig. 2. Effect of AVE0657 on pH_i in DVN neurons. A: Transmission light image of a dye-loaded slice under 10× magnification. The two white ovals indicate the DVN, located dorsal to the central canal (arrow). B and C: BCECF-AM-loaded DVN neurons (500 nm, red; 450 nm, green) before (B) and after 5 μmol/L AVE0657 application (C). Arrows indicate DVN neurons with fluorescence changes in response to AVE0657. D: Calibration curve for BCECF in individual DVN neurons. Each point represents the R_{fl} value at a given pH_i. E and F: The pH_i response to 5 μmol/L AVE0657 (E), compared with 0.05% DMSO (F).

of AVE0657 (5 μmol/L) for 1 to 2 min caused a rapid depolarization by 4.8 ± 1.1 mV in seven neurons, accompanied by an increase in firing rate to 4.1 ± 0.2 Hz (P <0.01, paired t test; n = 7). However, these effects were irreversible. In order to facilitate the effect of AVE0657 on pH_i, unbuffered pipette solution was used to compare the normalized membrane potential and firing rate with buffered pipette solution in response to equal concentrations of AVE0657. Although the average normalized membrane potential after the administration of AVE0657 was lower in the unbuffered condition, there was no significant difference between unbuffered (88.9 ± 2.3%, n = 4) and buffered conditions (91.0 ± 1.6%, n = 7) (P = 0.34, unpaired t test). However, more sensitive than the normalized membrane potential level, the normalized firing rate under unbuffered conditions resulted in a significantly greater increase (281.1 ± 18.6%) than the buffered condition (217.3 ± 33.5%) (P < 0.05, unpaired t test; n = 4/7 per group).

To determine the relationship between pH_e and pH_i in respiration-related neurons, we investigated the effect of AVE0657 on I_{so} and firing rate with or without acidified pH_e. As summarized in Fig. 4B and C, DVN neurons showed greater I_{so} responses to pH_e 7.1 + AVE0657 than to pH_e 7.1 alone (112 ± 19 pA *versus* 140 ± 13 pA, P <0.01, paired t test; n = 6). Besides, the firing rate was notably increased from 3.5 ± 0.2 Hz (pH_e 7.1) to 5.6 ± 0.4 Hz (pH_e 7.1 + AVE0657), P <0.01, paired t test; n = 6 (Fig. 4B, D). In addition, subtraction of the I-V relationships in pH_e 7.4 and pH_e 7.1 + AVE0657 showed a reversal potential at –91 ± 2 mV (n = 7), also close to the predicted K^+ equilibrium potential and fitted with the Goldman-Hodgkin-Katz equation (Fig. 4E).

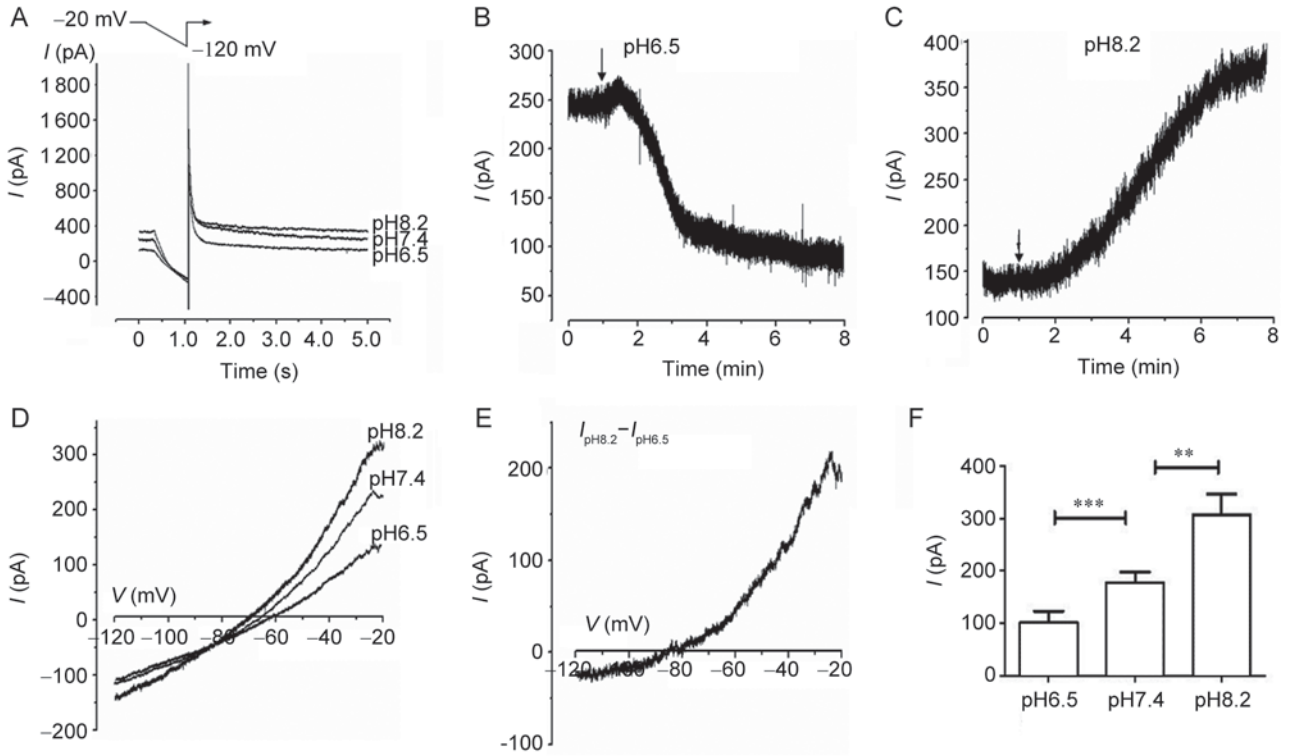

Fig. 3. I_{so} was modulated by acidification and/or alkalinization of pH_e. A: Current traces from hyperpolarizing voltage ramps applied to a DVN neuron subjected to different pH_e values in H-ACSF. Depolarization from –120 mV to –20 mV activated a large slowly-inactivating outward current. B and C: I_{so} measurements from a representative neuron voltage-clamped at −20 mV when subjected to acidified (B) or alkalized H-ACSF (C). Arrows indicate the time point of acidified or alkalized H-ACSF perfusion. D: Representative *I-V* relations from a DVN neuron obtained at different pH values. E: Current-voltage (*I-V*) relationships were subtracted (pH 8.2 minus pH 6.2) revealing that the pH-sensitive current was reversed at the predicted E_K and fitted with the Goldman-Hodgkin-Katz equation. F: Mean I_{so} at different pH_e values at –20 mV. **P <0.005; ***P <0.0005 (paired *t*-test).

DISCUSSION

Central respiratory chemoreceptors play a key role in sensing changes in P_{CO2} and/or pH in the brainstem and transforming them into homeostatic responses characterized by appropriate respiratory neuronal output. In the present study, we identified NHE-3 in the main chemosensitive regions of the brainstem. In DVN neurons, we measured both I_{so} and firing rate in response to different pH_e and/or pH_i, providing insight into the relationship between pH_e and pH_i and their roles in the chemosensitivity of respiratory neurons, as well as the reason why inhibition of NHE-3 increases ventilation.

TASK-like K^+ channels, members of the two-pore domain K^+ channel family[30] critical for sensing pH_e changes near the physiological range[28, 31], play a key role in determining neuronal resting membrane potential and regulating respiratory rhythm generation[32], as well as affecting the occurrence of spontaneous sleep apnea[20]. TASK-like K^+ channels have four properties that distinguish them from other known channels: selectivity for K^+, channel closure to extracellular acid, channel opening to extracellular alkali, and *I-V* relations described by the Goldman-Hodgkin-Katz equation. Here, we provided evidence that I_{so}, a pH-sensitive K^+ current that was further inhibited by AVE0657 after pH_e acidification, fully met the properties of TASK-like K^+ channels, implying a functional role of chemosensitivity in DVN neurons. It is generally believed that all three TASK channels (subtypes 1–3) are highly sensitive to pH_e, whereas the TASK-1 and TASK-2 channels contribute more to the I_{so} in DVN neurons because of their pKa values[28, 33, 34].

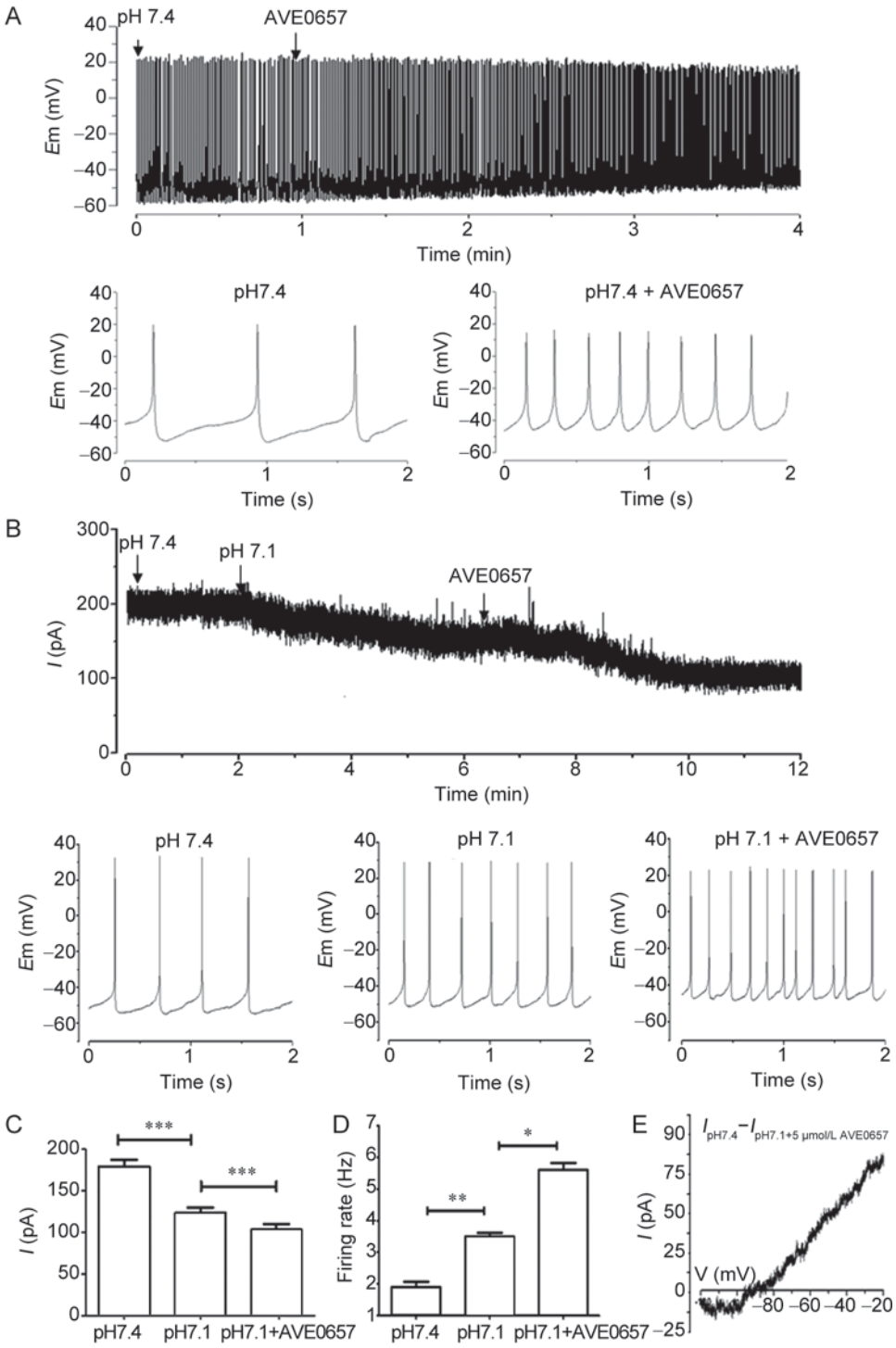

Fig. 4. Effects of AVE0657 on I_{so} and firing rate with buffered pipette solution. A: Administration of AVE0657 (5 μmol/L) resulted in rapid depolarization in a DVN neuron in H-ACSF (pH 7.4), accompanied by an increase in firing rate. Arrow indicates the time point of AVE0657 application. Below are 2-s samples of action potentials taken several minutes after the exposure to H-ACSF (left) and to AVE0657 (right). B: Time course of I_{so} in response to pH_e 7.1 and pH_e 7.1 + 5 μmol/L AVE0657. Arrows indicate the time points of acidified ACSF and AVE0657 application. Below are 2-s samples of action potentials taken several minutes after the exposure to each condition. C and D: Group mean ± SE data for I_{so} (C) and firing rate (D) in DVN neurons across pH 7.4, pH 7.1 and pH 7.1 + AVE0657 conditions. *P <0.01, **P <0.001, ***P <0.0005; ****P <0.00005 (paired t-test). E: Representative subtracted I-V relationships obtained with H-ACSF and AVE0657 in acidified H-ACSF.

By establishing a rough relationship between AVE0657 dose and pH_i, we chose 5 μmol/L AVE0657 for the following studies. We then found that 5 μmol/L AVE0657, with both buffered and unbuffered pipette solution, induced a rapid depolarization of membrane potential, accompanied by an increase in firing rate with a matched time-course of pH_i (in 2 min) observed with confocal microscopy. Moreover, equal concentrations of AVE0657 with unbuffered pipette solution excited DVN neurons to a greater extent than buffered pipette solution. Thus, we conclude that NHE-3 is active under normal pH_e, and AVE0657, a novel NHE-3 inhibitor, excites DVN neurons *via* a decrease in pH_i. All these characteristics of DVN neurons are consistent with the features shown by other chemosensitive neurons[15]. Coates *et al.*[7] demonstrated that pressure-injection of acetazolamide into the NTS/DVN produces a sphere of hypercapnia/acidosis with a radius of 300–350 μm, which increases ventilation and/or blood pressure, suggesting that central respiratory chemoreceptors reside in this region. The presence of individual chemosensitive neurons within the DVN was later confirmed by Huang *et al.* in an *in vitro* study[35]. Based on the NHE-3 distribution and DVN neuronal properties reported here and previous findings, we propose that the dorsal chemosensitive area in the medulla oblongata includes not only neurons in the vicinity of the NTS, but also neurons located in the DVN.

As our findings are related to the gas-exchange anomalies of obstructive sleep apnea, we limited the changes of pH_e within the physiological range of 7.4 to 7.1, instead of those found under other pathophysiological conditions such as stroke[36]. Ritucci *et al.*[37] provided evidence that, different from neurons in non-chemosensitive areas, those in chemosensitive areas do not exhibit pH_i recovery when exposed to hypercapnic acidosis or acidified pH_e. Our results demonstrated that application of AVE0657 still caused a further decrease of I_{so} and increase in the frequency of action potentials at a relatively steady state at pH_e 7.1. We therefore speculate that the activity of NHE-3 was not fully inhibited by the acidified H-ACSF at pH_e 7.1, and that this acidification merely resulted in a new steady-state of pH_i in DVN neurons. A recent study found that TASK-2 (but not TASK-1 and TASK-3) is activated by intracellular alkalinization and inhibited by intracellular acidification independently of pH_e *in vitro*[38]. Therefore, the further decrease in I_{so} after the application of AVE0657 was probably due to the inhibition of TASK-2 channels. According to the information provided by Sanofi-Aventis Pharmaceuticals, the specific NHE-3 inhibitor AVE0657 is 100 times more specific for NHE-3 than NHE-1 and NHE-2, from measurements in transfected fibroblasts. Due to confidentiality issues, the manufacturer did not provide detailed information on AVE0657. In the present study, nonspecific direct inhibition of TASK-like K^+ current by AVE0657 and cross-reaction among these three NHE subtypes cannot be excluded. However, as NHE-1 has been demonstrated in other chemosensitive regions such as the RTN, which mediates pH_i recovery[16], it is crucial to examine the expression of the other two NHE subtypes (NHE-1 and NHE-2), and determine the roles of each subtype and their relationships as pH-regulating transporters on DVN neurons in future.

TASK-1 and TASK-3 channels, which were once considered candidates for the determinant chemoreceptors of central respiratory chemical regulation, have been investigated in genetic experiments[39-41]. TASK-2 current keeps the membrane hyperpolarized to prevent a respiratory increase at low CO_2 concentrations, and hypercapnia successfully increases ventilation drive in wild-type mice but not in TASK-2 knockout mice[42]. However, the relevant depolarization in response to low CO_2 concentrations in the absence of TASK-2 implies that other factors such as NHE-3 and Kir channels are also involved in setting the threshold of the pH/CO_2 response. Why there are so many central chemosensitive sites, potential chemoreceptors and their variable locations (soma, dendrites and astrocytes)[35, 43, 44], involved in the regulation of respiratory control remains unanswered. Whether chemoreceptors interact with each other, and which chemoreceptor plays the predominant role need to be clarified.

In conclusion, extracellular and intracellular acidification have synergistic effect in the chemical control of respiration. Our results show that there might be a mechanism by which the decreased pH_i induced by inhibition of NHE-3 results in increased excitability of central chemosensitive respiratory neurons *via* inhibition of a pH-sensitive K^+ channel. The reduction in pH_e and pH_i may act in a synergistic or additive manner in regulating the

activity of central chemosensitive neurons.

ACKNOWLEDGEMENTS

We thank Dr. Qi-Hua He for technical assistance with confocal analysis. This work was supported by the National Natural Science Foundation of China (30900646 and 81241004).

Received date: 2013-01-15; Accepted date: 2013-03-12

REFERENCES

[1] Tregear S, Reston J, Schoelles K, Phillips B. Obstructive sleep apnea and risk of motor vehicle crash: systematic review and meta-analysis. J Clin Sleep Med 2009, 5: 573–581.

[2] Dempsey JA, Veasey SC, Morgan BJ, O'Donnell CP. Pathophysiology of sleep apnea. Physiol Rev 2010, 90: 47–112.

[3] Wang D, Marshall NS, Duffin J, Yee BJ, Wong KK, Noori N*, et al.* Phenotyping interindividual variability in obstructive sleep apnoea response to temazepam using ventilatory chemoreflexes during wakefulness. J Sleep Res 2011, 20: 526–532.

[4] Conrad SC, Nichols NL, Ritucci NA, Dean JB, Putnam RW. Development of chemosensitivity in neurons from the nucleus tractus solitarii (NTS) of neonatal rats. Respir Physiol Neurobiol 2009, 166: 4–12.

[5] Dean JB, Bayliss DA, Erickson JT, Lawing WL, Millhorn DE. Depolarization and stimulation of neurons in nucleus tractus solitarii by carbon dioxide does not require chemical synaptic input. Neuroscience 1990, 36: 207–216.

[6] Mulkey DK, Henderson RA, Putnam RW, Dean JB. Hyperbaric oxygen and chemical oxidants stimulate CO_2/H^+-sensitive neurons in rat brain stem slices. J Appl Physiol 2003, 95: 910–921.

[7] Coates EL, Li A, Nattie EE. Widespread sites of brain stem ventilatory chemoreceptors. J Appl Physiol 1993, 75: 5–14.

[8] Wellner-Kienitz MC, Shams H. CO_2-sensitive neurons in organotypic cultures of the fetal rat medulla. Respir Physiol 1998, 111: 137–151.

[9] Wang W, Richerson GB. Development of chemosensitivity of rat medullary raphe neurons. Neuroscience 1999, 90: 1001–1011.

[10] Solomon IC, Edelman NH, O'Neal MH 3rd. CO_2/H^+ chemoreception in the cat pre-Botzinger complex *in vivo*. J Appl Physiol 2000, 88: 1996–2007.

[11] Mulkey DK, Stornetta RL, Weston MC, Simmons JR, Parker A, Bayliss DA*, et al.* Respiratory control by ventral surface chemoreceptor neurons in rats. Nat Neurosci 2004, 7: 1360–1369.

[12] Oyamada Y, Ballantyne D, Muckenhoff K, Scheid P. Respiration-modulated membrane potential and chemosensitivity of locus coeruleus neurones in the *in vitro* brainstem-spinal cord of the neonatal rat. J Physiol 1998, 513 (Pt 2): 381–398.

[13] Ritucci NA, Chambers-Kersh L, Dean JB, Putnam RW. Intracellular pH regulation in neurons from chemosensitive and nonchemosensitive areas of the medulla. Am J Physiol 1998, 275: R1152–1163.

[14] Wiemann M, Baker RE, Bonnet U, Bingmann D. CO_2-sensitive medullary neurons: activation by intracellular acidification. Neuroreport 1998, 9: 167–170.

[15] Wiemann M, Schwark JR, Bonnet U, Jansen HW, Grinstein S, Baker RE*, et al.* Selective inhibition of the Na^+/H^+ exchanger type 3 activates CO_2/H^+-sensitive medullary neurones. Pflugers Arch 1999, 438: 255–262.

[16] Kersh AE, Hartzler LK, Havlin K, Hubbell BB, Nanagas V, Kalra A*, et al.* pH regulating transporters in neurons from various chemosensitive brainstem regions in neonatal rats. Am J Physiol Regul Integr Comp Physiol 2009, 297: R1409–1420.

[17] Kiwull-Schöne H, Wiemann M, Frede S, Bingmann D, Kiwull P. Tentative role of the Na^+/H^+ exchanger type 3 in central chemosensitivity of respiration. Adv Exp Med Biol 2003, 536: 415–421.

[18] Kiwull-Schöne H, Wiemann M, Frede S, Bingmann D, Wirth KJ, Heinelt U*, et al.* A novel inhibitor of the Na^+/H^+ exchanger type 3 activates the central respiratory CO_2 response and lowers the apneic threshold. Am J Respir Crit Care Med 2001, 164: 1303–1311.

[19] Kiwull-Schöne H, Teppema L, Wiemann M, Kalhoff H, Kiwull P. Pharmacological impact on loop gain properties to prevent irregular breathing. J Physiol Pharmacol 2008, 59: 37–45.

[20] Wang J, Zhang C, Li N, Su L, Wang G. Expression of TASK-1 in brainstem and the occurrence of central sleep apnea in rats. Respir Physiol Neurobiol 2008, 161: 23–28.

[21] Liu JS, Li JB, Gong XW, Gong HQ, Zhang PM, Liang PJ*, et al.* Spatiotemporal dynamics of high-K^+-induced epileptiform discharges in hippocampal slice and the effects of valproate. Neurosci Bull 2013, 29: 28–36.

[22] Ritucci NA, Erlichman JS, Dean JB, Putnam RW. A fluorescence technique to measure intracellular pH of single neurons in brainstem slices. J Neurosci Methods 1996, 68: 149–163.

[23] Fujita F, Uchida K, Moriyama T, Shima A, Shibasaki K, Inada H*, et al.* Intracellular alkalization causes pain sensation through activation of TRPA1 in mice. J Clin Invest 2008, 118: 4049–4057.

[24] Nattie E, Li A. Central chemoreception is a complex system

function that involves multiple brain stem sites. J Appl Physiol 2009, 106: 1464–1466.

[25] Gabriel A, Abdallah M, Yost CS, Winegar BD, Kindler CH. Localization of the tandem pore domain K^+ channel KCNK5 (TASK-2) in the rat central nervous system. Brain Res Mol Brain Res 2002, 98: 153–163.

[26] Preston A, Frydenberg M, Haynes JM. A1 and A2A adenosine receptor modulation of alpha 1-adrenoceptor-mediated contractility in human cultured prostatic stromal cells. Br J Pharmacol 2004, 141: 302–310.

[27] Hopwood SE, Trapp S. TASK-like K^+ channels mediate effects of 5-HT and extracellular pH in rat dorsal vagal neurones *in vitro*. J Physiol 2005, 568: 145–154.

[28] Bayliss DA, Talley EM, Sirois JE, Lei Q. TASK-1 is a highly modulated pH-sensitive 'leak' K^+ channel expressed in brainstem respiratory neurons. Respir Physiol 2001, 129: 159–174.

[29] Hille B. Ion Channels of Excitable Membranes. Sunderland: Sinauer Associates, 2001.

[30] Lesage F, Lazdunski M. Molecular and functional properties of two-pore-domain potassium channels. Am J Physiol Renal Physiol 2000, 279: F793–801.

[31] Duprat F, Lesage F, Fink M, Reyes R, Heurteaux C, Lazdunski M. TASK, a human background K^+ channel to sense external pH variations near physiological pH. EMBO J 1997, 16: 5464–5471.

[32] Koizumi H, Smerin SE, Yamanishi T, Moorjani BR, Zhang R, Smith JC. TASK channels contribute to the K^+-dominated leak current regulating respiratory rhythm generation *in vitro*. J Neurosci 2010, 30: 4273–4284.

[33] Talley EM, Lei Q, Sirois JE, Bayliss DA. TASK-1, a two-pore domain K^+ channel, is modulated by multiple neurotransmitters in motoneurons. Neuron 2000, 25: 399–410.

[34] Talley EM, Sirois JE, Lei Q, Bayliss DA. Two-pore-Domain (KCNK) potassium channels: dynamic roles in neuronal function. Neuroscientist 2003, 9: 46–56.

[35] Huang RQ, Erlichman JS, Dean JB. Cell-cell coupling between CO_2-excited neurons in the dorsal medulla oblongata. Neuroscience 1997, 80: 41–57.

[36] Tombaugh GC, Somjen GG. Effects of extracellular pH on voltage-gated Na^+, K^+ and Ca^{2+} currents in isolated rat CA1 neurons. J Physiol 1996, 493 (Pt 3): 719–732.

[37] Ritucci NA, Dean JB, Putnam RW. Intracellular pH response to hypercapnia in neurons from chemosensitive areas of the medulla. Am J Physiol 1997, 273: R433–441.

[38] Niemeyer MI, Cid LP, Pena-Munzenmayer G, Sepulveda FV. Separate gating mechanisms mediate the regulation of K2P potassium channel TASK-2 by intra- and extracellular pH. J Biol Chem 2010, 285: 16467–16475.

[39] Linden AM, Aller MI, Leppa E, Vekovischeva O, Aitta-Aho T, Veale EL*, et al*. The *in vivo* contributions of TASK-1-containing channels to the actions of inhalation anesthetics, the alpha(2) adrenergic sedative dexmedetomidine, and cannabinoid agonists. J Pharmacol Exp Ther 2006, 317: 615–626.

[40] Mulkey DK, Talley EM, Stornetta RL, Siegel AR, West GH, Chen X*, et al*. TASK channels determine pH sensitivity in select respiratory neurons but do not contribute to central respiratory chemosensitivity. J Neurosci 2007, 27: 14049–14058.

[41] Trapp S, Aller MI, Wisden W, Gourine AV. A role for TASK-1 (KCNK3) channels in the chemosensory control of breathing. J Neurosci 2008, 28: 8844–8850.

[42] Gestreau C, Heitzmann D, Thomas J, Dubreuil V, Bandulik S, Reichold M*, et al*. Task2 potassium channels set central respiratory CO_2 and O_2 sensitivity. Proc Natl Acad Sci U S A 2010, 107: 2325–2330.

[43] Fukuda Y, Honda Y, Schläfke ME, Loeschcke HH. Effect of H+ on the membrane potential of silent cells in the ventral and dorsal surface layers of the rat medulla *in vitro*. Pflugers Arch 1978, 376: 229–235.

[44] Gourine AV, Kasymov V, Marina N, Tang F, Figueiredo MF, Lane S*, et al*. Astrocytes control breathing through pH-dependent release of ATP. Science 2010, 329: 571–575.